Criteria for Shear Banding in Time-Dependent Flows of Complex Fluids

Robyn L. Moorcroft and Suzanne M. Fielding

Department of Physics, Durham University, Science Laboratories, South Road, Durham DH1 3LE, United Kingdom

We study theoretically the onset of shear banding in the three most common time-dependent rheological protocols: step stress, finite strain ramp (a limit of which gives a step strain), and shear startup. By means of a linear stability analysis we provide a fluid-universal criterion for the onset of banding for each protocol, which depends only on the shape of the experimentally measured time-dependent rheological response function, independent of the constitutive law and internal state variables of the particular fluid in question. Our predictions thus have the same highly general status, in these time-dependent flows, as the widely known criterion for banding in steady state (of negatively sloping shear stress vs shear rate). We illustrate them with simulations of the Rolie-Poly model of polymer flows, and the soft glassy rheology model of disordered soft solids.

PACS numbers: 83.10.−y, 83.50.Ax

Many complex fluids show shear banding [1], in which an initially homogeneous sample of fluid separates into layers of differing viscosity under an applied shear flow. Examples include surfactants [2], polymers [3], soft glassy materials [4,5], and (possibly) bioactive fluids [6]. At a fundamental level shear banding can be viewed as a nonequilibrium, flow-induced phase transition, or equivalently as a hydrodynamic instability of viscoelastic origin. In practical terms it drastically alters the rheology (flow response) of these materials and thus impacts industrially in plastics, foodstuffs, well-bore fluids, etc.

In steady state, the criterion for shear banding is (usually [7]) that the underlying constitutive relation between shear stress Σ and shear rate $\dot{\gamma}$ for homogeneous flow has negative slope, $d\Sigma/d\dot{\gamma} < 0$. However most practical flows involve a strong time dependence, whether perpetually or during a startup process in which a steady flow is established from an initial rest state. Data in polymers [8–15], surfactants [16–18], soft glasses [19–22], and simulations [23–30] reveal that shear bands often also arise during these time-dependent flows, and can be sufficiently long-lived to represent the ultimate flow response of the material for practical purposes, even if the constitutive curve is monotonic, $d\Sigma/d\dot{\gamma} > 0$.

In view of these widespread observations, crucially lacking is any known criterion for the onset of banding in time-dependent flows. This Letter provides such criteria, with the same fluid-universal status as the criterion given above in steady state: independent of the internal constitutive properties of the particular fluid in question, and depending only on the shape of the experimentally measured rheological response function. It does so for each of the three most common time-dependent experimental protocols: step stress, finite strain ramp, and shear startup. Our aim is thereby to develop a unified understanding of experimental observations of time-dependent shear banding, and to facilitate the design of flow protocols that optimally enhance or mitigate it as desired.

The criteria are derived via a linear stability analysis performed within a highly general framework that encompasses most widely used models for the rheology of polymeric fluids (polymers solutions, melts and wormlike micelles) and soft glassy materials (foams, dense emulsions, colloids, etc.). These general analytical results are then illustrated by simulations of two specific models: the Rolie-Poly (RP) model of polymeric fluids [31], and the soft glassy rheology (SGR) model [27,32].

Throughout we assume incompressible flow, with mass balance $\nabla \cdot \boldsymbol{v} = 0$. We also assume the flow to be inertialess, with force balance $0 = \nabla \cdot \boldsymbol{\Sigma} = \nabla \cdot (\boldsymbol{\sigma} + 2\eta \boldsymbol{D} - p\boldsymbol{I})$. Here p is the pressure field and $\boldsymbol{v}$ the fluid velocity, with symmetrized strain rate tensor $\boldsymbol{D} = \frac{1}{2}(\boldsymbol{K} + \boldsymbol{K}^T)$, in which $\boldsymbol{K}_{\alpha\beta} = \partial_\beta v_\alpha$. This generalizes Stokes' equation of creeping flow such that any fluid element carries a Newtonian stress $2\eta \boldsymbol{D}$ of viscosity η, as in a simple fluid, and a viscoelastic stress $\boldsymbol{\sigma}$ from the internal mesoscopic substructures in a complex fluid: emulsion droplets, polymer chains, etc.

Following standard practice we write $\boldsymbol{\sigma} = G\boldsymbol{W}$, with G an elastic modulus and $\boldsymbol{W}$ a dimensionless conformation tensor characterizing the deformation of these mesoscopic substructures. The dynamics of $\boldsymbol{W}$ in flow are prescribed by a rheological constitutive model for the particular fluid in question. The criteria for shear banding presented below are derived in a generalized framework [33] that includes most commonly used constitutive models as special cases. However, for pedagogical purposes we develop our arguments initially within the specific context of the RP model [31] of polymeric flows, which has:

$$\dot{\boldsymbol{W}} + \boldsymbol{v} \cdot \nabla \boldsymbol{W} = \boldsymbol{K} \cdot \boldsymbol{W} + \boldsymbol{W} \cdot \boldsymbol{K}^T - \frac{1}{\tau_D}(\boldsymbol{W} - \boldsymbol{I})$$

$$- \frac{2}{\tau_R}(1 - A)[\boldsymbol{W} + \beta A^{-2\delta}(\boldsymbol{W} - \boldsymbol{I})]. \quad (1)$$

Here $A = \sqrt{3/\mathrm{tr}\mathbf{W}}$. The terms in $\mathbf{v}$ and $\mathbf{K}$ describe advection by flow, which drives $\mathbf{W}$ away from undeformed equilibrium. ($\mathbf{W} = \mathbf{I}$ in a well rested fluid.) The remaining terms model relaxation back to equilibrium: τ_D is the time scale for a chainlike polymer molecule to escape its entanglements with other molecules, and τ_R is the (much faster) time scale on which any stretching of the chain relaxes [34]. For convenience below we often take the nonstretch limit $\tau_R/\tau_D \to 0$, but comment on the robustness of our results to this. Following [31] we set $\delta = -1/2$ throughout.

We consider a sample of fluid sandwiched between parallel plates at $y = \{0, L\}$, well rested for times $t < 0$ then sheared for $t > 0$ in one of the time-dependent protocols defined below: step stress, finite strain ramp or shear startup. The upper plate moves in the $\hat{\mathbf{x}}$ direction and the flow is assumed unidirectional, with fluid velocity $\mathbf{v} = v_x(y, t)\hat{\mathbf{x}}$ and shear rate $\dot{\gamma}(y, t) = \partial_y v_x$. Spatial heterogeneity (banding) is allowed in the flow gradient direction $\hat{\mathbf{y}}$ only, with translational invariance in $\hat{\mathbf{x}}$, $\hat{\mathbf{z}}$.

The nonstretch RP model then gives, componentwise

$$\Sigma(t) = GW_{xy}(y, t) + \eta\dot{\gamma}(y, t),$$
$$\partial_t W_{xy}(y, t) = f(W_{xy}, W_{yy}, \dot{\gamma}),$$
$$\partial_t W_{yy}(y, t) = g(W_{xy}, W_{yy}, \dot{\gamma}),$$
(2)

with $f = \dot{\gamma}[W_{yy} - \frac{2}{3}(1+\beta)W_{xy}^2] - \frac{1}{\tau_D}W_{xy}$, $g = \frac{2}{3}\dot{\gamma}[\beta W_{xy} - (1+\beta)W_{xy}W_{yy}] - \frac{1}{\tau_D}(W_{yy}-1)$. Inertialess flow demands uniform total shear stress: $\Sigma = \Sigma(t)$ only. Our numerics use units in which $L = 1$, $\tau_D = 1$, $G = 1$.

Step stress.—Consider first a sample subject to a step stress $\Sigma(t) = \Sigma_0\Theta(t)$ where Θ is the Heaviside step function. If the fluid's response to this applied load were one of homogeneous shear, this would be prescribed by the spatially uniform but time-dependent solution of (2): $\dot{\gamma} = \dot{\gamma}_0(t)$, $\mathbf{W} = \mathbf{W}_0(t)$. Differentiating (2) shows any such homogeneous state to obey

$$0 = G\dot{W}_{0xy} + \eta\ddot{\gamma}_0,$$
$$\ddot{W}_{0xy} = \frac{\partial f}{\partial W_{xy}}\dot{W}_{0xy} + \frac{\partial f}{\partial W_{yy}}\dot{W}_{0yy} + \frac{\partial f}{\partial\dot{\gamma}}\ddot{\gamma}_0,$$
(3)
$$\ddot{W}_{0yy} = \frac{\partial g}{\partial W_{xy}}\dot{W}_{0xy} + \frac{\partial g}{\partial W_{yy}}\dot{W}_{0yy} + \frac{\partial g}{\partial\dot{\gamma}}\ddot{\gamma}_0,$$

subject to the initial condition $\dot{\gamma}_0(0) = \Sigma_0/\eta$, $\dot{W}_{0xy} = f(0, 1, \Sigma_0/\eta)$, $\dot{W}_{0yy} = g(0, 1, \Sigma_0/\eta)$.

We now examine whether any such state of uniform shear becomes linearly unstable to the onset of banding at any time during its evolution. To do so we express the full response to the applied load as a sum of this underlying homogeneous "base state" plus an (initially) small heterogeneous perturbation: $\dot{\gamma}(y, t) = \dot{\gamma}_0(t) + \sum_n \delta\dot{\gamma}_n(t)\cos(n\pi y/L)$, $\mathbf{W}(y, t) = \mathbf{W}_0(t) + \sum_n \delta\mathbf{W}_n(t)\cos(n\pi y/L)$. Substituting into (2) shows that, to first order in $\delta\dot{\gamma}_n$, $\delta\mathbf{W}_n$, the perturbations obey

$$0 = G\delta W_{nxy} + \eta\delta\dot{\gamma}_n,$$
$$\delta\dot{W}_{nxy} = \frac{\partial f}{\partial W_{xy}}\delta W_{nxy} + \frac{\partial f}{\partial W_{yy}}\delta W_{nyy} + \frac{\partial f}{\partial\dot{\gamma}}\delta\dot{\gamma}_n,$$
(4)
$$\delta\dot{W}_{nyy} = \frac{\partial g}{\partial W_{xy}}\delta W_{nxy} + \frac{\partial g}{\partial W_{yy}}\delta W_{nyy} + \frac{\partial g}{\partial\dot{\gamma}}\delta\dot{\gamma}_n.$$

These must be solved subject to source terms specifying the seeding of any heterogeneity, whether due to (i) sample preparation, (ii) slight flow device curvature, (iii) mechanical or thermal noise. We consider (i), using an initial condition $\delta\mathbf{W}_n(0) = \epsilon_n\mathbf{N}_n$, small ϵ_n, and the entries of $\mathbf{N}_n$ drawn from a distribution of mean 0 and width 1.

Equations (3) and (4) together show that the *heterogeneous* fluctuations $\delta\mathbf{W}_n$, $\delta\dot{\gamma}_n$ obey the same dynamics as the time derivative of the *homogeneous* base state $\mathbf{W}_0$, $\dot{\gamma}_0$ [35]. Shear bands must therefore develop (growing $|\delta\dot{\gamma}_n|$) whenever

$$\frac{d^2\dot{\gamma}_0}{dt^2}\bigg/\frac{d\dot{\gamma}_0}{dt} > 0.$$
(5)

This criterion is written in terms of the time derivatives of the creep curve $\gamma_0(t)$ of the underlying base state in our stability analysis. How does this $\gamma_0(t)$ relate to the bulk creep curve $\gamma(t)$ that is measured experimentally by recording the movement of the rheometer plates? Clearly, before any banding develops $\gamma_0(t) = \gamma(t)$ by definition. Accordingly the onset of banding out of a state of initially homogeneous creep should happen once the experimentally measured $\gamma(t)$ likewise obeys (5).

Figure 1 shows our numerical results for the nonstretch RP model, with parameters for which the constitutive curve $\Sigma(\dot{\gamma})$ is monotonic and the steady state homogeneous. Figure 1(a) shows a representative time-differentiated creep curve for homogeneous flow $\dot{\gamma}_0(t)$. The regime of instability to banding as predicted by (5), where $\dot{\gamma}_0(t)$ simultaneously shows upward slope and curvature, is shown dashed. A full nonlinear simulation of the RP model indeed confirms time-dependent shear banding in this regime [Figs. 1(b) and 1(c)], with homogeneous flow recovered in steady state.

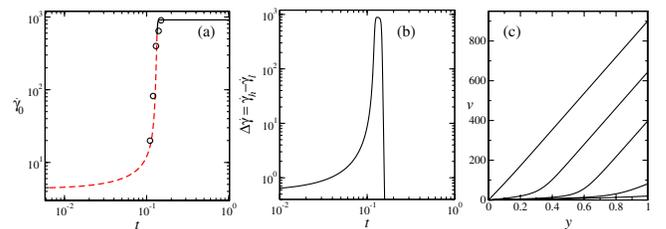How general is this criterion (5)? Clearly Eqs. (2)–(5) make no assumption about the functional forms of f, g,

FIG. 1 (color online). Nonstretch RP model: $\beta = 0.8$, $\eta = 10^{-4}$, $\Sigma_0 = 0.7$. (a) Time derivative of creep curve. Dashed line: linearly unstable regime. (b) Corresponding degree of banding (difference in maximum and minimum shear rate across cell). (c) Flow profiles at times marked by circles in (a) for $\epsilon_n = 0.1\delta_{n,1}$, $l = 10^{-2}$.

and so must apply to any differential constitutive model with $d = 2$ dynamical state variables (W_{xy} and W_{yy} above). This is easily extended [33] to arbitrary d, to allow for the dynamics of other (e.g., normal) stress components, fluidity variables in a soft glass, ordering tensors in a liquid crystal, etc. Accordingly our criterion (5) should hold for *any* constitutive model of differential form. Taking $d \to \infty$ extends this to systems with infinitely many state variables and so, we now also argue, those governed by *integral* constitutive models, of which the SGR model of disordered soft solids is an example.

Accordingly we now simulate the SGR model [32] in a form capable of addressing banded flows [27,33]. We focus on its glass phase $x < 1$ where the constitutive curve has a yield stress with monotonic increase beyond: $\Sigma(\dot\gamma) = \Sigma_y + c\dot\gamma^{1-x}$. For an applied stress just above Σ_y we see a long regime of slow creep $\dot\gamma \sim t^{-x} t_w^{x-1}$, with t_w the sample age before loading. See Fig. 2(a). (Experimentally microgels show $\dot\gamma \sim t^{-2/3}$ [21], reminiscent of Andrade creep for plastically deforming crystals [36].) This slow creep ends in a transition to a regime of upward slope $\partial\dot\gamma/\partial t > 0$ and curvature $\partial^2\dot\gamma/\partial t^2 > 0$ in which shear bands form [Figs. 2(b) and 2(c)], consistent with (5). Subsequent inflexion to downward curvature $\partial^2\dot\gamma/\partial t^2 < 0$ defines a fluidization time $t_f \sim t_w(\Sigma - \Sigma_y)^{-\alpha}$ with $\alpha = O(1)$, after which the system recovers homogeneous flow in steady state. Microgel experiments [21] likewise show $t_f \sim (\Sigma - \Sigma_y)^{-\beta}$ with concentration-dependent β.

We therefore finally propose (5) as a universal criterion for shear banding following an imposed step shear stress. It is consistent with numerous experiments on polymers [9–12,16–18,37] and soft glassy materials [21,22].

Finite strain ramp.—Consider next a well rested sample subject to a rapid strain ramp $\gamma_0 = \dot\gamma_0 t$ by moving the upper plate at speed $\dot\gamma_0 L$ for times $0 < t < t^*$, after which the strain is held constant at $\gamma_0^* = \dot\gamma_0 t^*$. Taking $\dot\gamma_0 \to \infty$,
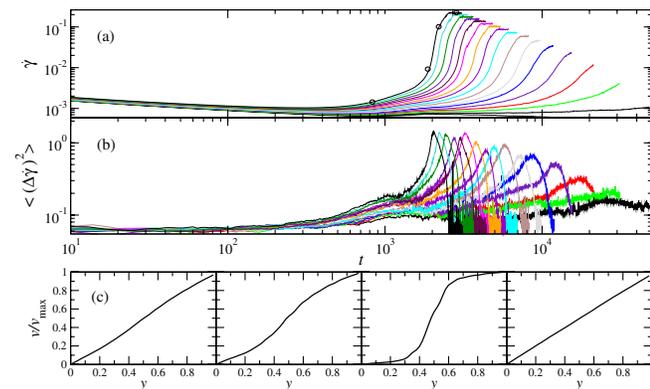

FIG. 2 (color online). SGR model: (a) Differentiated creep curves for stress values $\Sigma_0/\Sigma_y = 1.005, 1.010, \ldots, 1.080$ (curves upwards). (b) Corresponding degree of banding. (c) Normalized velocity profiles for the circles in (a). $x = 0.3$, $w = 0.05$, $n = 50$, $m = 10000$. Initial sample age $t_w = 10^3[1 + \epsilon\cos(2\pi y)]$, $\epsilon = 0.1$.

$t^* \to 0$ at fixed γ_0^* gives a true step strain. As above we shall study this initially in the nonstretch RP model, before generalizing to other materials.

We start by rewriting (2) in a form that emphasizes its additive loading and relaxation dynamics:

$$\Sigma(t) = GW_{xy}(y, t) + \eta\dot\gamma(y, t),$$
$$\partial_t W_{xy}(y, t) = \dot\gamma S(W_{xy}, W_{yy}) - \frac{1}{\tau_D}W_{xy}, \tag{6}$$

with $S = W_{yy} - \frac{2}{3}(1 + \beta)W_{xy}^2$. (The equation for W_{yy} is not needed here.) Within this we consider first a state of idealized homogeneous response to the imposed strain. This will then form the base state in a stability analysis for the onset of banding below. To best approximate a true step strain we focus on a fast ramp $\dot\gamma\tau_D \gg 1$. During any such ramp the base state stress obeys

$$\frac{d\Sigma_0}{d\gamma_0} = GS(W_{0xy}, W_{0yy}) \quad \text{for } \dot\gamma\tau_D \gg 1. \tag{7}$$

Postramp, it relaxes back to equilibrium as $\dot\Sigma_0 = -\Sigma_0/\tau_D$.

For the fast ramps studied here no banding develops during the ramp itself. To investigate whether the sample can remain homogeneous during its relaxation back to equilibrium, or whether it instead transiently bands during it, we add initially small heterogeneous perturbations to the relaxing base state: $\dot\gamma(y, t) = \sum_n \delta\dot\gamma_n(t)\cos(n\pi y/L)$, $W(y, t) = W_0(t) + \sum_n \delta W_n(t)\cos(n\pi y/L)$. Substituting these into (6) shows that, to first order, the perturbations evolve postramp as

$$\frac{d\delta\dot\gamma_n}{dt} = -\frac{G}{\eta}S(W_{0xy}, W_{0yy})\delta\dot\gamma_n \quad \text{for } \eta \ll G\tau. \tag{8}$$

Denoting by (W_{0xy}^*, W_{0yy}^*) the system's state instantaneously as the ramp ends at time t^*, and noting the state to be continuous at t^*, we combine (7) and (8) to show that the perturbations, immediately postramp, obey

$$\left.\frac{d\delta\dot\gamma_n}{dt}\right|_{t=t^{*+}} = \omega\delta\dot\gamma_n \quad \text{with } \omega = -\frac{1}{\eta}d\Sigma_0/d\gamma_0|_{t=t^{*-}}. \tag{9}$$

This shows that shear bands will start developing immediately following a fast strain ramp if the stress had been decreasing with strain just prior to the ramp ending

$$d\Sigma_0/d\gamma_0|_{t=t^{*-}} < 0. \tag{10}$$

This result accords with early intuition [38]. It can be shown to hold quite generally [33] for all fluids with additive loading and relaxation dynamics (including the RP model with chain stretch reinstated).

Numerical results for the RP model support this prediction: Fig. 3. The lower curve is for a fast ramp in the nonstretch model. This has nonlinear loading dynamics, $S = W_{yy} - \frac{2}{3}(1 + \beta)W_{xy}^2$, so during ramp behaves as a nonlinear elastic solid with a maximum of stress vs strain. If the total applied strain γ^* exceeds this, the system is left
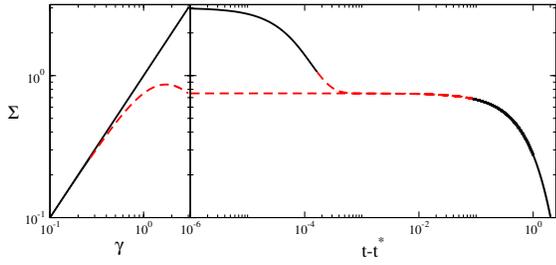
FIG. 3 (color online).   Left: Stress vs strain for a fast ramp in the RP model. $\beta = 0.0$, $\tau_R = 10^{-4}$, $\eta = 10^{-5}$. Right: Relaxation postramp; unstable region in a dashed line. Upper curve: Appreciable chain stretch, $\tau_R \dot{\gamma} \to \infty$. Lower: Negligible stretch, $\tau_R \dot{\gamma} = 0.1$.

unstable to banding immediately postramp. The upper curve shows a fast ramp in the full model with chain stretch. This has linear loading dynamics, $S = W_{yy}$, and during ramp acts as a linear elastic solid. Accordingly it is stable against banding immediately afterwards. However this upper curve reveals further important polymer physics. Relaxation of chain stretch on the time scale τ_R postramp restores a state as if no stretch had arisen in the first place: the upper curve rejoins the lower, both are unstable to banding and only finally decay on the time scale τ_D. This is consistent with experiments [13–15,39] and numerics [24,26] showing that bands can form either straight after a step strain, or following an induction period. In extensional equivalent it might also underlie the physics of delayed necking [40,41].

The SGR model has linearly increasing stress in a fast ramp so is stable against banding after it.

Shear startup.—Consider finally, shear applied at constant rate $\dot{\gamma}_0$ for all times $t > 0$, giving strain $\gamma_0 = \dot{\gamma}_0 t$. This protocol is discussed here in outline only, with details elsewhere [42]. Our aim is to discover in what regions of the plane $(\dot{\gamma}_0, \gamma_0)$ the fluid is unstable to banding (Fig. 4). Any horizontal slice across this plane corresponds to the system's evolution in a single startup run at fixed $\dot{\gamma}_0$, to
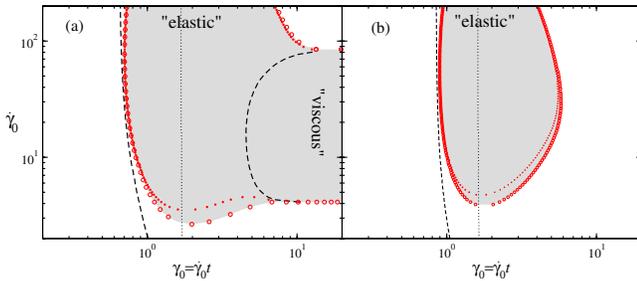

FIG. 4 (color online).   Shear startup in the Rolie-Poly model. Unstable region shaded. (a) Nonmonotonic constitutive curve, $\beta = 0.4$, $\tau_R = 0.0$, $\eta = 10^{-4}$. Large circles: Full onset criterion. Right dashed line delimits viscous criterion (11). Left dashed line: Elastic criterion (12). Small circles: Elastic plus viscous terms (12) + (11). Dotted line: stress overshoot $\partial_{\gamma_0}\Sigma_0 = 0$. (b) Corresponding figure for monotonic constitutive curve, $\beta = 1.0$.

steady state in the limit $\dot{\gamma}_0 t = \gamma_0 \to \infty$. A vertical slice at the far right-hand side corresponds to the fluid's steady state properties as a function of $\dot{\gamma}_0$.

Our calculation [33] proceeds as usual by considering a base state of homogeneous response to this applied shear, then deriving a criterion [43] for when this becomes unstable to banding. This contains derivatives of the base state's stress signal $\Sigma_0(\gamma_0, \dot{\gamma}_0)$ (which, as discussed above, corresponds to the experimental signal $\Sigma(\gamma, \dot{\gamma})$ at least until appreciable bands develop).

In a thought experiment in which the flow is artificially constrained to stay homogeneous until it attains steady state in the limit $\gamma_0 \to \infty$, this criterion [43] reduces to the known "viscous" instability for steady state bands:

$$\partial_{\dot{\gamma}_0}\Sigma_0|_{\gamma_0} < 0, \qquad (11)$$

apparent along a vertical slice at the right of Fig. 4(a).

More importantly our criterion [43] also applies to *finite* times t and strains $\gamma_0 = \dot{\gamma}_0 t$. It therefore predicts at what stage *during* startup banding first sets in, according to the shape of the stress signal as a function of strain during startup. Indeed when sheared at a very high rate $\dot{\gamma}_0 \to \infty$, many materials effectively act as nonlinear elastic solids, with a stress vs strain curve that attains a unique limiting function $\Sigma_0(\gamma_0)$, independent of $\dot{\gamma}_0$. In any such case our criterion [43] reduces to a purely "elastic" banding instability, onset once

$$A\partial_{\gamma_0}\Sigma_0|_{\dot{\gamma}_0} + \dot{\gamma}_0 \partial^2\Sigma_0/\partial\gamma_0^2|_{\dot{\gamma}_0} < 0 \quad \text{with} \quad A > 0. \qquad (12)$$

The first term, taken alone, predicts onset just after any overshoot $\partial_{\gamma_0}\Sigma_0 = 0$ in the stress vs strain signal. The second term corrects this, causing onset just before overshoot. This is indeed apparent along a horizontal slice at high strain rate in Fig. 4(a). Equation (12) holds for any model with $d = 2$ state variables. See Ref. [33] for $d > 2$.

For a fluid with a monotonic constitutive curve, $\partial_{\dot{\gamma}_0}\Sigma_0 > 0$, steady state instability is absent. See Fig. 4(b). However a patch of elasticlike instability remains. This shows that shear bands can arise transiently, as predicted by (12), associated with an overshoot in the stress startup curve $\Sigma_0(\gamma_0)$, even if absent in steady state.

Accordingly experimentalists should be alert to the generic tendency to shear banding in any material that shows an overshoot in stress vs strain $\Sigma(\gamma)$ during startup. This may or may not persist to steady state depending on the slope of the ultimate flow curve $\Sigma(\dot{\gamma})$. These results are consistent with numerous experimental [8,10,16,18] and simulation [23,24,26,30] studies.

Conclusion.—We have given universal criteria for shear banding in time-dependent flows of complex fluids. In step stress, banding is predicted if the creep response curve obeys $(\partial^2\dot{\gamma}/\partial t^2)/(\partial\dot{\gamma}/\partial t) > 0$. In a finite strain ramp, bands start developing immediately postramp if the stress had been decreasing with strain by the end of the ramp. In shear startup we find separate "viscous" and "elastic"

instabilities for a broad category of fluids that attain a limiting stress startup curve $\Sigma(\gamma_0)$ in fast flows. We hope our predictions will help unify the understanding of widespread data for time-dependent flows, and stimulate further experiments and simulations of other models (e.g., Ref. [44]) to test our ideas further.

---

[1] P. D. Olmsted, Rheol. Acta **47**, 283 (2008); S. Manneville, *ibid.* **47**, 301 (2008).

[2] S. Lerouge and J.-F. Berret, in *Polymer Characterization*, Advances in Polymer Science Vol. 230, edited by K. Dusek and J.-F. Joanny (Springer, Berlin and Heidelberg, 2010), pp. 1–71; M. E. Cates and S. M. Fielding, Adv. Phys. **55**, 799 (2006).

[3] P. Tapadia and S.-Q. Wang, Phys. Rev. Lett. **96**, 016001 (2006).

[4] G. Ovarlez, S. Rodts, X. Chateau, and P. Coussot, Rheol. Acta **48**, 831 (2009).

[5] P. Coussot, Q. Nguyen, H. Huynh, and D. Bonn, J. Rheol. **46**, 573 (2002).

[6] M. E. Cates, S. M. Fielding, D. Marenduzzo, E. Orlandini, and J. M. Yeomans, Phys. Rev. Lett. **101**, 068102 (2008).

[7] This applies for single component fluids (or multicomponent ones without strong flow-concentration coupling) in the absence of strong memory effects.

[8] S. Ravindranath, S.-Q. Wang, M. Olechnowicz, and R. P. Quirk, Macromolecules **41**, 2663 (2008).

[9] Y. T. Hu, L. Wilen, A. Philips, and A. Lips, J. Rheol. **51**, 275 (2007).

[10] P. E. Boukany and S.-Q. Wang, J. Rheol. **53**, 73 (2009).

[11] P. Tapadia and S.-Q. Wang, Phys. Rev. Lett. **91**, 198301 (2003).

[12] S. Ravindranath and S.-Q. Wang, J. Rheol. **52**, 957 (2008).

[13] P. E. Boukany, S.-Q. Wang, and X. Wang, Macromolecules **42**, 6261 (2009).

[14] S.-Q. Wang, S. Ravindranath, P. Boukany, M. Olechnowicz, R. P. Quirk, A. Halasa, and J. Mays, Phys. Rev. Lett. **97**, 187801 (2006).

[15] P. E. Boukany and S.-Q. Wang, Macromolecules **42**, 2222 (2009).

[16] Y. T. Hu, C. Palla, and A. Lips, J. Rheol. **52**, 379 (2008).

[17] P. E. Boukany and S.-Q. Wang, Macromolecules **41**, 1455 (2008).

[18] Y. T. Hu and A. Lips, J. Rheol. **49**, 1001 (2005).

[19] T. Divoux, C. Barentin, and S. Manneville, Soft Matter **7**, 9335 (2011).

[20] T. Divoux, D. Tamarii, C. Barentin, and S. Manneville, Phys. Rev. Lett. **104**, 208301 (2010).

[21] T. Divoux, C. Barentin, and S. Manneville, Soft Matter **7**, 8409 (2011).

[22] T. Gibaud, D. Frelat, and S. Manneville, Soft Matter **6**, 3482 (2010).

[23] J. M. Adams, S. M. Fielding, and P. D. Olmsted, J. Rheol. **55**, 1007 (2011).

[24] J. M. Adams and P. D. Olmsted, Phys. Rev. Lett. **102**, 067801 (2009); O. S. Agimelen and P. D. Olmsted, arXiv:1204.4169.

[25] M. L. Manning, J. S. Langer, and J. M. Carlson, Phys. Rev. E **76**, 056106 (2007).

[26] L. Zhou, P. A. Vasquez, L. P. Cook, and G. H. McKinley, J. Rheol. **52**, 591 (2008).

[27] R. L. Moorcroft, M. E. Cates, and S. M. Fielding, Phys. Rev. Lett. **106**, 055502 (2011).

[28] M. L. Manning, E. G. Daub, J. S. Langer, and J. M. Carlson, Phys. Rev. E **79**, 016110 (2009).

[29] E. A. Jagla, J. Stat. Mech. (2010) P12025.

[30] J. Cao and A. E. Likhtman, Phys. Rev. Lett. **108**, 028302 (2012).

[31] A. Likhtman and R. Graham, J. Non-Newtonian Fluid Mech. **114**, 1 (2003).

[32] P. Sollich, F. Lequeux, P. Hébraud, and M. E. Cates, Phys. Rev. Lett. **78**, 2020 (1997).

[33] See the Supplemental Material at http://link.aps.org/supplemental/10.1103/PhysRevLett.110.086001 for details of the RP and SGR models, and the outline of a theoretical framework that shows the stability criteria to be fluid universal.

[34] In principle diffusive terms $D\nabla^2 W$ must also be added to the right-hand side of Eq. (1) to prohibit flow heterogeneity at scales smaller than the fluid microstructure $l = \sqrt{D\tau}$. In our linear stability analysis these can be neglected for the fluctuations of interest, with wavelength $\gg l$.

[35] Due to their different initial conditions they are not guaranteed to evolve colinearly. Numerically, though, we find they always do become colinear after a short transient.

[36] M. C. Miguel, A. Vespignani, M. Zaiser, and S. Zapperi, Phys. Rev. Lett. **89**, 165501 (2002); H. Nechad, A. Helmstetter, R. El Guerjouma, and D. Sornette, Phys. Rev. Lett., **94**, 045501 (2005).

[37] Y. T. Hu, J. Rheol. **54**, 1307 (2010).

[38] G. Marrucci and N. Grizzuti, J. Rheol. **27**, 433 (1983).

[39] Y. Fang, G. Wang, N. Tian, X. Wang, X. Zhu, P. Lin, G. Ma, and L. Li, J. Rheol. **55**, 939 (2011).

[40] A. Lyhne, H. K. Rasmussen, and O. Hassager, Phys. Rev. Lett. **102**, 138301 (2009).

[41] Y. Wang, S. Q. Wang, P. Boukany, and X. Wang, Phys. Rev. Lett. **99**, 237801 (2007).

[42] R. L. Moorcroft and S. M. Fielding (to be published).

[43] The instability criterion in startup is $\partial_{\dot{\gamma}_0}\Sigma_0|_{\dot{\gamma}_0} - \boldsymbol{p} \cdot \boldsymbol{M}^{-1} \cdot [\partial_{\gamma_0}\boldsymbol{s}|_{\dot{\gamma}_0} + \dot{\gamma}_0 \partial_{\dot{\gamma}_0}\partial_{\gamma_0}\boldsymbol{s}] < 0$. Here $\boldsymbol{s}$ is a vector comprising all dynamical state variables, $\boldsymbol{M}$ a matrix formed by linearing the dynamics of these state variables, and $\boldsymbol{p}$ a projection vector. See the Supplemental Material [33] for details.

[44] P. Coussot, and G. Ovarlez, Eur. Phys. J. E **33**, 183 (2010); K. Martens, L. Bocquet, and J. L. Barrat, Soft Matter **8**, 4197 (2012).